Applied Catalysis B: Environmental 115–116 (2012) 169–178

Contents lists available at SciVerse ScienceDirect

Applied Catalysis B: Environmental

journal homepage: www.elsevier.com/locate/apcatb

Pore size tuning of functionalized SBA-15 catalysts for the selective production of furfural from xylose

I. Agirrezabal-Telleria*, J. Requies, M.B. Güemez, P.L. Arias

Department of Chemical and Environmental Engineering, Engineering School of the University of the Basque Country, Alameda Urquijo s/n, 48013, Bilbao, Spain

ARTICLE INFO

Article history:
Received 7 November 2011
Received in revised form 9 December 2011
Accepted 15 December 2011
Available online 24 December 2011

Keywords:
Furfural
Xylose-dehydration
Functionalized
SBA-15
Aging

ABSTRACT

Furfural (FUR) is widely used as an industrial solvent and can be potentially used as building-block to produce added-value products, such as methyltetrahydrofuran (MeTHF) or levulinic acid. It is currently manufactured from pentosan-rich biomass via steam-stripping under homogeneously catalyzed conditions. Alternatives focus on novel process optimization or on the design of heterogeneous water-tolerant Brönsted acids. In this work, functionalized SBA-15 catalysts with controlled textural properties were prepared in order to study their performance during xylose cyclodehydration. The combination of these two procedures allowed to selectively produce FUR from xylose. Preliminary catalyst screening at 140 °C showed a FUR selectivity maxima for the material aged at 100 °C. Moreover, the results revealed a direct influence of the sulfonic load and the reaction temperature on the catalytic performance of SBA-15 samples. Promising results were achieved for the propylsulfonic SBA-15 aged at 100 °C, since it could optimize the FUR yield up to 82% at 170 °C of reaction temperature. Finally, the stability of the catalysts in different solvents and their regeneration were also evaluated.

© 2011 Elsevier B.V. All rights reserved.

1. Introduction

The upgrading of lignocellulosic biomass wastes into fuels and higher added-value chemicals is one the most researched topics in the forthcoming concept of biorefinery. The production of second generation fuels can directly affect the feasibility of integrated strategies to use lignocellulosic wastes as energy sources [1]. In this sense, dehydration reactions of carbohydrates in the biomass lead to interesting furan molecules. Furfural (FUR), manufactured from pentosan-rich biomass, is used as a building-block in order to produce new generation biofuels (methyltetrahydrofuran (MeTHF)), furan resins or as an industrial solvent [2,3].

During the initial stage of FUR production, the pentosan in the hemicellulose are hydrolyzed to pentose carbohydrates, which are subsequently cyclodehydrated to furfural. Industrially, these reactions are catalyzed using concentrated sulfuric or phosphoric acid. In order to minimize FUR loss through secondary reactions, it is simultaneously removed from the reacting medium using superheated steam as the stripping agent [4]. Alternative homogeneous catalysts include acetic acid, superphosphate or sulfate salts [5,6]. However, coke formation due to yield-loss reactions leads to low FUR selectivity especially at high pentose conversions. Moreover, all these processes suffer from corrosion issues, toxic effluents and high stripping costs, difficulting further separation and recycling stages [7]. Recent FUR manufacturing-process optimization studies are focused on increasing reaction temperatures up to 250 °C and rapid quenching of the reaction products by flash decompression [8]. In a previous publication [9], our study focused on the conversion of xylose to FUR catalyzed by Amberlyst 70 ion-exchange resin and simultaneous nitrogen-stripping. This work achieved furfural-rich stripped streams with almost 100% FUR purity and even biphasic water/furfural separation at high initial xylose concentration loads.

Biomass conversion and xylose dehydration research activities focus on the synthesis of novel water-tolerant heterogeneous acid catalysts due to the ease of post-reaction separation [1,10–12]. The characteristics of the studied catalysts feature high Brönsted acidity and adequate textural properties in order to study the xylose conversion mechanism and optimize the FUR production yield. Valente and co-workers reported various possible catalysts, ranging from exfoliated metal oxides [13], modified mesoporous silicas [14–16], conventional sulfated bulk zirconia [17] and silicoaluminophosphates [18]. Xylose conversion reactions were carried out using monophasic dimethylsulfoxide (DMSO) or toluene as the extracting solvent in biphasic systems. Moreover, high shape selectivity was achieved using zeolitic structures adjusted to the reacting molecule size [7]. Moreau et al. obtained high FUR selectivity (90%) at low xylose conversions using zeolitic structures such H-mordenite [19].

In the catalytic field, micelle-templated mesoporous materials have shown high reaction activity for the upgrading of biomass

* Corresponding author. Tel.: +34 617912295; fax: +34 946014179.
E-mail address: iker_agirrezabal@ehu.es (I. Agirrezabal-Telleria).

0926-3373/$ – see front matter © 2011 Elsevier B.V. All rights reserved.
doi:10.1016/j.apcatb.2011.12.025

to fuels [20]. The concept of supramolecular chemistry was first proposed suggesting that molecules can self-organize into defined structures using weak interactions such as hydrogen bonding. This idea was first applied for mesoporous materials to synthesize the so-called M41S structures [21]. The organic–inorganic hybrid approach was extended (under acidic conditions – HCl), for triblock nonionic copolymers as structure directing agents (SDAs) to create the SBA-15 materials [22]. These ordered mesoporous materials show high surface area (>700 m^2/g), high pore volume (>0.7 cm^3/g) and pore sizes in the range of 20–150 Å. Additionally, the cooperative assembly of silica and hydrophilic–hydrophobic micelles enables to tune the textural properties by varying the synthesis conditions. Ternary systems using co-surfactants [23], HCl/H_3PO_4 mixtures [24] or aging temperature-control [25–27] allow micropore–mesopore structure tuning for the reduction of non-desired products and thus higher product selectivity [28]. Moreover, the cylindrical shape of the pores allows fast molecule diffusion into them.

Several modified SBA-15 supports were reported in the field of catalytic reactions [29,30] and biomass upgrading [31–33] with high hydrothermal stability. This concept was also applied to the dehydration reaction of xylose. Shi et al. [34] used Al-promoted SO_4^{2-}/ZrO_2/SBA-15 materials showing high number and intensity of acid sites. On the other hand, different functionalized SBA-15 supports have been catalytically proved as promising [35]. Recently, propylsulfonic SBA-15 catalysts achieved 92% xylose conversion and 74% FUR selectivity at high toluene/water ratios [36]. However, no work has been focused on the concept of pore-size adjustment combined with SBA-15 sulfonation for the selective dehydration of xylose to FUR.

The aim of this work is therefore to prepare different functionalized SBA-15 materials with controlled textural-properties by varying the synthesis aging-temperature. Since water is the preferred solvent for xylose dehydration, the synthesized materials and their active sites should be adequate for reactions under the presence of water. Moreover, reducing the particle size to nanoscale would increase the surface-area to pore-volume ratio and limit the diffusion path lengths of xylose to the reaction site, which may avoid secondary product formation. This paper discusses the catalytic performance of functionalized SBA-15 catalysts for the dehydration of xylose to FUR using solvents such as DMSO and biphasic systems of toluene/water. Controlled pore size and xylose/furfural diffusion control should selectively optimize the final FUR yield. Finally, catalyst stability and regeneration will also be evaluated.

2. Experimental

2.1. Sample preparation

2.1.1. Arenesulfonic SBA-15 via co-condensation

The arenesulfonic groups were incorporated into SBA-15 supports following the recipe described in the literature [35]: 4 g of Pluronic 123 (PEO-PPO-PEO copolymer – *Aldrich*) were first dissolved in 125 mL of HCl (1.9 M) at room temperature. The solution was heated to 40 °C before the dropwise addition of tetraethylorthosilicate (TEOS – *Aldrich*). A prehydrolysis time of 180 min was established. The sulfonic precursor CSPTMS (2-(4-chlorosulfonylphenyl)ethyltrimethoxysilane – *Acros Organics*) was added at once together with the oxidizing agent (H_2O_2 30 wt.% – *Aldrich*). The molar composition of the mixture for 4 g of P123 was 0.0369 TEOS:0.0041 CSPTMS:0.0123 H_2O_2:0.24 HCl:6.67 H_2O. This way, a CSPTMS/(TEOS + CSPTMS) ratio of 0.10 was set. The resulting solution was hydrolyzed at 40 °C for 20 h under stirring and it was later transferred into a Teflon lined autoclave for aging. The aging conditions were set at 100 °C for 24 h under static conditions. The solid product was recovered by filtration, washed thoroughly with water and dried at room temperature. The P123 template present in the silica structure was extracted with ethanol under reflux (1.5 g of as-synthesized material per 400 mL of ethanol). The solid product was filtered, washed with ethanol and dried. This material was named as A100-0.10.

2.1.2. Propylsulfonic SBA-15 materials via co-condensation

These materials were prepared following the recipe described in the literature [37]. The procedure was the same as in Section 2.1.2, except for the addition of MPTMS (mercaptopropyltrimethoxysilane – *Aldrich*) as the sulfonic group precursor. The molar composition of the mixture for 4 g of P123 was 0.0369 TEOS:0.0041 MPTMS:0.0738 H_2O_2:0.24 HCl:6.67 H_2O. Same MPTMS/(TEOS + MPTMS) ratio of 0.10 was set. The silica precursor was hydrolyzed at 40 °C for 20 h and aged at different conditions. In order to study the structural changes, the aging-temperature was increased 10 °C for each material from 80 °C to 120 °C for 24 h under static conditions. Filtration and solvent extraction procedures were the same as previously described. The nomenclature of the samples is as follows: for example, P100-0.10 for an aging-temperature of 100 °C.

2.1.3. Propylsulfonic SBA-15 functionalized by post-oxidation

These materials were prepared at an aging-temperature of 100 °C using the same procedure as described in Section 2.1.2, except for the addition of the H_2O_2 during the hydrolysis period. After solvent extraction, the immobilized MPTMS groups were oxidized with H_2O_2. Typically, 0.3 g of as-extracted wet material was suspended in 10 g of 30 wt.% H_2O_2 and stirred at room temperature in a N_2 atmosphere for 5 h. The resulting solid material was filtered and washed with ethanol. Finally, the wet material (1 wt.%) was suspended in 1 M H_2SO_4 for 2 h at room temperature. The solid product, named as P100P-0.10, was filtered again, washed with ethanol and dried.

2.2. Sample characterization

Nitrogen physisorption isotherms of as-extracted SBA-15 materials were obtained at 77 K over the whole range of relative pressures, using an Autosorb 1C (Quantachrome) automatic device and samples previously degassed at 423 K for 12 h. The specific surface area was calculated using the Brunauer–Emmett–Teller (S_{BET}) method while the micropore volume was estimated by the *t*-plot method. The pore size distribution (PSD), the total pore volume (V_P) and pore diameter (D_P) were derived using the Barrett–Joyner–Halenda (BJH) method.

Thermogravimetric analysis (TGA) of fresh and used SBA-15 catalysts was performed in the TGA/SDTA 851e module (Mettler-Toledo), measuring the weight variation during oxidation at a heating ramp of 10 °C min^{-1} from room temperature until 800 °C.

XRD data were collected on a Bruker D8 Advance diffractometer equipped with a Cu tube, Ge(1 1 1) incident beam monochromator (λ = 1.5406 Å) (fixed slit 1 mm) and a Sol-X energy dispersive detector (fixed slit 0.05 mm). The sample was mounted on a zero background silicon wafer embedded in a generic sample holder. Data were collected from 0.3 to 5° 2θ (step size = 0.01 and time per step = 20 s) at RT. A variable divergence and antiscattering slit (V4) giving a constant area of sample illumination of 4 mm was used.

Ion-exchange capacities (mmol $H^+/g\ SiO_2$) of the functionalized mesoporous materials were determined using 0.05 M of tetramethylammonium chloride (TMACl) as exchange agent. In a typical measurement, 0.05 g of SBA-15 material was suspended in 10 g of the mentioned solution and equilibrated for 18 h. The resulting

Table 1
Physicochemical properties and catalytic activity of functionalized SBA-15 materials for the dehydration of xylose to furfural.

Catalyst	Catalyst characterization				Toluene/water[b]				DMSO[b]			
	S_{BET} (m^2/g)	V_P (cm^3/g)	Main D_P (Å)	Acidity[c] (mmol H^+/g)	X_X[d] (%)	FUR_S[e] (%)	r_0'[f] (mmol g_{cat} h^{-1})	TOF (mmol (meq $H^+)^{-1}$ h^{-1})	X_X[d] (%)	FUR_S[e] (%)	r_0'[f] (mmol g_{cat} h^{-1})	TOF (mmol (meq $H^+)^{-1}$ h^{-1})
None	–	–	–	–	43	25	–	–	90	23	–	–
Amberlyst 70	–	–	–	2.55	65	49	1.21	0.47	99	37	1.84	0.72
A100-0.10[a]	931	1.35	82.1	1.17	63	60	1.20	1.00	99	45	1.84	1.57
P100-0.10[a]	1129	1.85	74.2	1.04	67	82	1.25	1.19	97	61	1.80	1.74
P100P-0.10[a]	574	0.67	50.3	0.62	45	40	0.83	1.35	92	24	1.71	2.76

[a] Organosiloxane initial molar loading = 0.10(MPTMS/MPTMS + TEOS).
[b] Reaction conditions: 200 mL, 140 °C, 2 wt.% xylose loading and 60 wt.% catalyst loading with respect to initial xylose. $SD_{TOL/W}$ = 5%, SD_{DMSO} = 3%.
[c] Measured by TMACl equilibration followed by titration with NaOH.
[d] Conversion of xylose after 20 h.
[e] Selectivity to FUR after 20 h.
[f] Initial rate calculated after 8 h of reaction.

Table 2
Physicochemical properties of propylsulfonic SBA-15 materials synthesized at different aging-temperatures.

	S_{BET} (m^2/g)	V_P (cm^3/g)	$V_{\mu P}$ (cm^3/g)	Main D_P (Å)	Mean D_P (Å)	Wall thickness[b] (Å)	d_{100}[c] (Å)	Acidity TMACl[d] (mmol $H^+/g\,SiO_2$)	Acidity TGA[e] (mmol H^+/SiO_2)
P80-0.10[a]	736	0.74	0.1300	39.2	40.6	79.5	104	1.00	1.15
P90-0.10[a]	721	0.96	0.0300	74.3	53.6	64.2	102	1.01	1.04
P100-0.10[a]	1129	1.85	0.0020	74.2	65.7	61.3	110	1.04	1.12
P110-0.10[a]	839	1.55	0.0004	81.5	74.2	43.6	102	1.21	1.20
P115-0.10[a]	598	1.05	0.0021	70.4	74.9	56.7	114	1.04	1.12
P120-0.10[a]	712	1.41	0.0010	74.2	79.2	45.5	108	1.23	1.25

[a] Organosiloxane initial molar loading = 0.10(MPTMS/MPTMS + TEOS).
[b] Calculated by a_0 – pore diameter ($a_0 = 2d_{100}/\sqrt{3}$).
[c] d_{100} spacing derived from XRD patterns.
[d] Materials equilibrated with TMACl and titrated with 0.01 M NaOH.
[e] Measured from propylsulfonic weight loss during TGA oxidation analysis.

solution was titrated potentiometrically by dropwise addition of 0.01 M NaOH.

2.3. Catalytic tests

Xylose dehydration catalytic tests were performed in a 200 mL temperature-controlled stain-steel reactor stirred at 500 rpm (applying Maers' criterion [(page 379), Ref. 38], the limitation associated to external diffusion can be neglected). The system was pressurized at 10 bar in order to keep the reaction medium in liquid-phase. Once the reaction solvent was heated up until the temperature of study, the corresponding xylose solution was pumped with a Waters 515 pump to obtain an initial xylose load of 20 g/L. Catalyst load was fixed at 60 wt.% with respect to initial xylose load and reaction time was set at 20 h. In order to study the stability of functionalized SBA-15, the solid catalysts were recovered by filtration, washed thoroughly with ethanol and dried.

The products and the remaining xylose were quantified using a HPLC module ICS-3000 from DIONEX coupled to an AS40 Autosampler. FUR was quantified using a Kinetex C18-XB 150 mm × 4.6 mm column from Phenomenex at 40 °C and coupled to a UV-2070 Plus detector from JASCO at 280 nm wavelength. The mobile phase was pumped at 1 mL min^{-1} and consisted of 0.01 M H_2SO_4 and 10% (v/v) acetonitrile aqueous solution. Xylose was quantified using a CarboPac PA20 3 mm × 150 mm column, at 30 °C and 0.5 mL min^{-1}, using 8 mM of NaOH as mobile phase. Detection was performed using an electrochemical cell, with integrated amperometry and Standard Carbohydrate Quad method.

The definition of xylose conversion (X_X), FUR selectivity (FUR_S) and FUR yield (FUR_Y) are as follows:

$$X_X(\%) = 1 - (\text{mol of xylose at time } t)/(\text{initial xylose mol})$$
$$FUR_S(\%) = \text{mol of FUR at time } t/\text{mol xylose converted}$$
$$FUR_Y(\%) = X_X \times FUR_S$$

3. Results and discussion

3.1. Screening of functionalized SBA-15

The SBA-15 supports were modified using three different sulfonation methods: an arenesulfonic precursor via co-condensation and a propylsulfonic precursor via co-condensation and post-oxidation. This preliminary catalyst screening aimed to choose the most efficient sulfonation method for xylose dehydration and later extend this study to more detailed pore size adjustments. These catalysts were first tested under batch conditions using toluene/water biphasic extraction systems at 1:1 (v/v) ratios. FUR is miscible in toluene (as indicated by Lima et al. [7], the partition ratio for furfural in toluene/water at room temperature is around 8–10). So lower toluene/water ratios than in the literature were here considered. Moreover, xylose was also dehydrated using DMSO as the single solvent. DMSO has been proved as a promising solvent for the conversion of different carbohydrates even in combination with sulfonic mesoporous materials [14]. The reaction temperature was set at 140 °C in order to reduce auto-resinification and condensation reaction effects in the reaction medium.

Table 1 summarizes the physicochemical characteristics of the mentioned catalysts. According to N_2 physisorption data, the presence of arenesulfonic precursors by co-condensation created materials with lower structural development (S_{BET} = 931 m^2/g, D_P = 82.1 Å) compared to the propylsulfonic precursor (S_{BET} = 1129 m^2/g, D_P = 74.2 Å). Apparently, the interactions between silica and bigger aryl molecules increased the pore size during the mesophase formation. However, post-oxidation with H_2O_2 (P100P-0.10) gave higher structural instability. It seemed that the synthesis conditions during co-condensation were milder than post-oxidation, where the harsh oxidizing conditions with H_2O_2 and the aggressive dehydrating conditions with H_2SO_4 shrank the silica matrix considerably (D_P = 46.7 Å).

If catalytic behavior in toluene/water medium of the different samples is compared using initial rates (r'_0) when deactivation effects can be neglected (see Table 1), the most active one is the P100-0.10 (1.25 mmol g_{cat}^{-1} h^{-1}), even if the differences are not too high. These initial rates are of the same order of magnitude as the one experimentally determined for the ion-exchange resin Amberlyst 70. From these initial rate data and the acidity of fresh materials, the corresponding TOF values were estimated. The P100P-0.10 contained the most active sites followed by P100-0.10, A100-0.10 and Amberlyst 70 (1.35 > 1.19 > 1.00 > 0.47 h^{-1}). It can be concluded that the material originated through a post-oxidation stage, showed lower acidity but its acid sites were more active. As observed in Table 1, this trend was also observed when DMSO was used as solvent.

As observed in Table 1, non-catalyzed systems showed low X_X and FUR_S values, while the presence of a strong ion-exchange sulfonic resin (Amberlyst 70) dehydrated xylose at higher rates but also catalyzed secondary reactions on the surface. Among the rest of the catalysts, the acid sites generated from sulfonic aryl or propyl precursors showed different catalytic activities. Even if A100-0.10 and P100-0.10 present similar acid capacities around 1 mmol H^+/g SiO_2, the propyl acid sites seemed to be more selective for FUR. This difference might also be attributed to a better surface-area development for the P100-0.10 sample. The A100-0.10 might have higher acid concentration per surface area unit, enhancing furfural yield-loss reactions. On the other hand, the poor structural development and the low acid capacity of P100P-0.10 were also reflected on the low FUR_S. For all these differences, this study was further extended to the influence of structural aspects of propylsulfonic SBA-15 on the xylose dehydration catalytic activity.

3.2. Pore size tuning of propylsulfonic catalysts

3.2.1. Catalyst characterization

As mentioned in Section 3.1, the propylsulfonic SBA-15 supports synthesized via co-condensation allowed the highest FUR_S during xylose dehydration. One of the main goals of this paper is focused on adjusting the SBA-15 pore size by aging-temperature to selectively optimize FUR production.

During the micelle formation of SBA-15 synthesis, poly(ethylene oxide) surfactant tails protrude from the poly(propylene oxide) core and interact between each other. These will be penetrated into the silica matrix. If the aging-temperature is increased, then PEO is partially dehydrated and the volume of the hydrophilic corona is reduced. Based on literature data, SBA-15 silica aged at 35 °C exhibits thick pore walls and micropores that are too short to connect adjacent mesoporous channels [39]. As the synthesis aging-temperature increases to 80–100 °C, the pore walls become thinner and the mesoporous channels become connected by micro/meso bridges. Micropore fraction shows a maximum at 80 °C (24 h), and at even higher temperature (130 °C), the micropores tend to vanish completely. However, the diameter of the mesopores tends to increase gradually with the aging-temperature [25]. As a result, aging-temperature was varied 10 °C from 80 °C to 120 °C for each material containing propylsulfonic acid sites. The decomposition temperature of P123 block copolymer is close to 130 °C, so last two aging-temperatures were set at 115 °C and 120 °C.

During SBA-15 synthesis, the silica matrix development was barely affected by the incorporation of propylsulfonic precursors. N_2 physisorption data confirmed a typical mesoporous type IV isotherm. When comparing different samples, the S_{BET} values

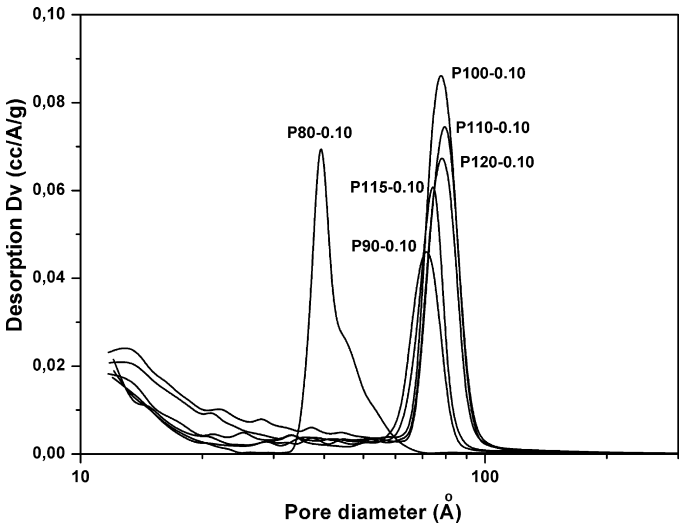

Fig. 1. Pore size distribution obtained from N_2 physisorption data of different propylsulfonic SBA-15 samples.

showed a maximum centered at P100-0.10, while these values decreased considerably for the rest of materials (see Table 2). Low aging-temperatures (P80-0.10/P90-0.10) developed structures with lower accessibility (~720 m^2/g), whereas the fast micelle arrangement rate for samples over 120 °C showed a drop in the total surface area. On the other hand, P90-0.10 and P100-0.10 samples showed similar pore volume maxima centered at 74 Å (see Fig. 1). However, high polymerization temperatures (P100-0.10) seemed to generate higher surface area than P90-0.10 in the whole porous structure, reaching S_{BET} values up to 1129 m^2/g. Among the materials aged over 100 °C, the pore diameters (Main D_P) at V_P maxima were centered ~75 Å, but pore volume at this D_P was considerably lower for samples such as P115-0.10 and P120-0.10. In general, average Mean D_P was proportionally increased with aging-temperature, while the microporous fraction showed an inverse effect. Mesoporous wall structure had also a similar trend: lower aged materials showed lower silica polymerization degrees but thicker pore walls, while materials aged at higher temperatures produced stronger structures (see Fig. A1 NMR data) with thinner mesopore walls. Compared to other silica-based mesoporous structures (MCM41), the presence of thicker pore walls on SBA-15 (50–70 Å) provides higher hydrothermal stability.

According to the TGA data presented in Fig. 2, the extracted materials prepared via co-condensation showed two prominent desorption peaks. The first one due to the adsorption of water on the silica matrix, and a second one, centered at 490 °C, due to the desorption of propylsulfonic acid sites. The quantitative determinations of the propylsulfonic weight loss were in good agreement with the initial precursor incorporation. Such thermal stability was not evidenced for Amberlyst 70, showing a decomposition peak starting at 260 °C. Ethanol seemed to be an efficient extraction solvent for the majority of mesopores, even if residual copolymer could be detected by 13CP NMR detection (Fig. A2), probably at micropore levels.

The crystallinity of as-synthesized materials was checked by XRD analysis (Fig. 3a). The X-ray patterns of extracted materials showed in general three typical SBA-15 type reflections centered at (1 0 0), (1 1 0) and (2 0 0). P80-0.10 and P90-0.10 materials showed lower crystallinity compared to P100-0.10. On the other hand, materials synthesized over 100 °C presented lower mesoscopic ordering. This might be attributed to a higher silica polymerization rate during aging or even due to higher P123 micelle interactions at high aging-temperatures. As a result, the d_{100} spacing (interpore distance) was also increased with the aging-temperature.

Finally, Table 2 represents the acidity values of different as-synthesized materials. The ion-exchange capacities, carried out by means of acid site equilibration with TMACl and subsequent acid-base titration, were in good agreement with the TGA decomposition values. By using different equilibration agents, several studies sustained the presence of sulfonic acid sites on the surface of mesoporous channels rather than on the microporous corona [35]. In our case, most of propylsulfonic SBA-15 materials showed an acid capacity in the order of 1 mmol $H^+/g\,SiO_2$. Even more important, no significant correlation between acidity and aging-temperature was observed. This study takes advantage of this fact in order to evaluate the porous structure effect on the catalytic activity rather than the acid capacity.

3.2.2. Xylose dehydration activity

In the first instance, as-synthesized propylsulfonic samples were catalytically tested in water at 140 °C, since it is the cheapest and the most abundant solvent during the dehydration of the pentosan present in the biomass. Later on, the experiments were also carried out in toluene/water and DMSO.

Fig. 4 summarizes the conversion and selectivity data for the materials aged from 80 to 120 °C. As mentioned in Section 3.2.1, N_2 physisorption data of propylsulfonic materials showed clear evidences of different structural development during aging. This effect was also reflected on the FUR_S of propylsulfonic catalysts. Materials such as P80-0.10 achieved smaller pore diameters and lower surface development. Thus at the given reaction temperature, xylose diffusion was limited by the catalyst pore size, leading to low FUR production. Comparing water and DMSO solvents, it seemed that most of dehydration and secondary reactions for P80-0.10 occurred in the DMSO phase (FUR_S 35% in DMSO and 48% in water), since it showed lower selectivity than P90-0.10/P100-0.10 at nearly same xylose conversion (99%). Even if DMSO has a higher pK_a (35) than water (15), xylose molecule dehydration seems to be slower in water. On the other hand, more accessible structures such as P100-0.10 selectively produced FUR to reach final FUR_S of 62% in DMSO and 56% in water. Among the samples with similar Main D_P, P100-0.10 performed better than P90-0.10. As well as in Section 3.1, P100-0.10 acid sites might be more uniformly dispersed all over the silica surface area, reducing the oligomers production rate in the pores. The low FUR_S achieved with P110-0.10 and P120-0.10 might not be attributed to an increase in their acid content (1.2 mmol $H^+/g\,SiO_2$), but to more accessible pores where diffusion path lengths and xylose/furfural contact times were increased, leading to drops in FUR_S. On the other hand, the use of toluene as the extracting agent improved the final product selectivity up to 82% for the P100-0.10 sample. Same FUR_S improvement was observed for the rest of samples. Given the toluene extraction efficiency, the FUR_S variation was not as clear as in water or DMSO, but a similar FUR_S maximum was observed for the propylsulfonic sample series.

The effective diffusion coefficient was calculated based on Knudsen and molecular diffusivity [(pages 454–461), Ref. 40]. The molecular diffusivity (D_{MOL}) between water/xylose or water/furfural showed small differences around, 0.180 cm^2/s (see Table A1). However, the Knudsen coefficient (D_K) for FUR is increased from 0.041 cm^2/s for P80-0.10 to 0.079 cm^2/s for P120-0.10. The D_K of xylose presents a similar behavior. As a result, the effective FUR diffusivity constant was increased from 0.033 to 0.054 cm^2/s for P80-0.10 and P120-0.10, respectively. It has to be noted that aging enhances the sulfonic–silica interactions. P120-0.10 acid sites might be more stable during time, and thus could extend the xylose conversion longer. This property, together with the diffusion effect on samples such as P120-0.10, might explain

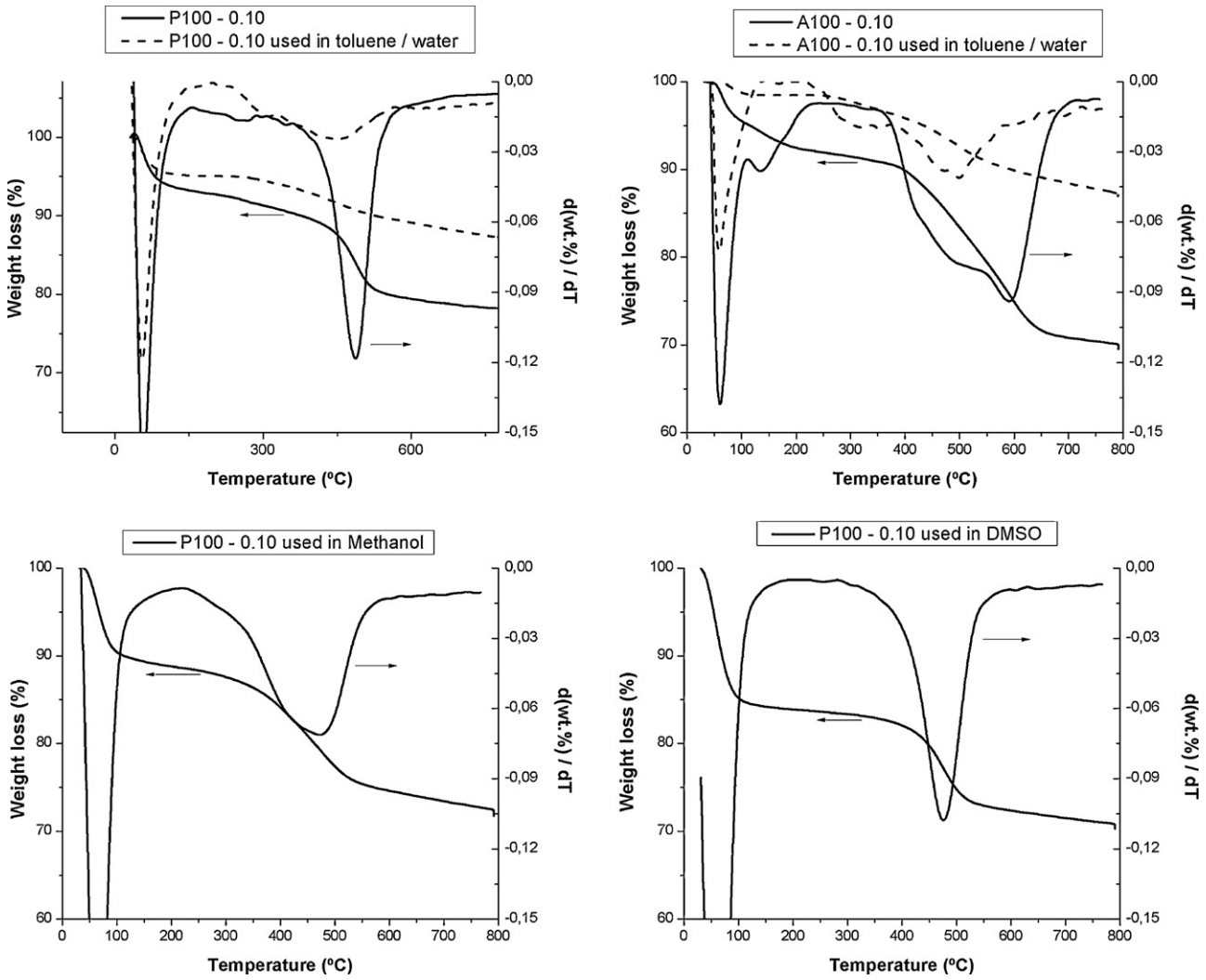

Fig. 2. TGA data of fresh and used propylsulfonic SBA-15 and arenesulfonic SBA-15.

the X_X differences in water-phase reactions for the series of propylsulfonic SBA-15 materials.

As mentioned in Section 3.2.1, there is still residual copolymer present in the ethanol-extracted materials. This surfactant is mostly present in micropores, since ethanol accesses easier to the mesopores than to micropores. During catalyst testing, xylose and furfural diffusivities are limited by the pore size: $D_{K,FUR}$ = 0.012 cm^2/s for a micropore of 12 nm, whereas the $D_{K,FUR}$ for a mesopore of 70 nm is 0.070 cm^2/s. This suggests that most of xylose dehydration activity occurred on the mesopore surface. As previously mentioned, the development of mesopores and surface area showed considerable influence on the overall xylose conversion and FUR selectivity. Thus, the presence of micropores had lower influence than the aging temperature on the final catalytic performance.

As a brief conclusion, samples with big mesopores (P110-0.10/P120-0.10) increased the xylose conversion rate because of higher diffusivity but this molecular mobility enhanced yield-loss reactions, as well. On the other hand, samples such as P80-0.10 showed higher selectivity at 140 °C but were not capable of dehydrating xylose at similar reaction rates. For this reason, samples such as P90-0.10/P100-0.10 seemed to optimize the conversion/selectivity balance. In general, these values were comparable to other mesoporous materials [14,16] or zeolitic structures [19,41] tested during xylose dehydration. However, the batchwise performance in single water-phase conditions is still low.

3.3. Organosiloxane loading

Once the SBA-15 structure was optimized (P100-0.10), and in order to evaluate the acid-site uniformity over propylsulfonic acids, the influence of sulfonic loading on P100 was tested. High organosiloxane loadings seem to affect directly the micelle-silica interactions during aging, so two other samples were synthesized at (MPTMS/TEOS + MPTMS) molar ratios of 0.05 and 0.20. The surface properties were similarly preserved (S_{BET} ~ 1100 m^2/g and Main D_P = 75 Å), since the sulfonic loading at these levels barely affects the mesophase formation. As checked in the literature [37], the presence of high organosiloxane loadings at same initial $P123/H_2O_2$ ratios does not lead to residual non-oxidized thiol groups (appearing at ~28 ppm). T^m/Q^n ratio obtained from 29Si NMR data confirmed that the sulfonic incorporation corresponds to the initial mixture. According to 13C CPMAS data (see supplementary information), the P100-0.20 spectrum did not seem to have extra resonances due to incomplete thiol oxidation. This difference was also reflected on the acid-exchange capacity (summarized in Table 3).

As observed in Table 3, the calculated TOF values for the sulfonic P100 materials proved that less acid samples contained more

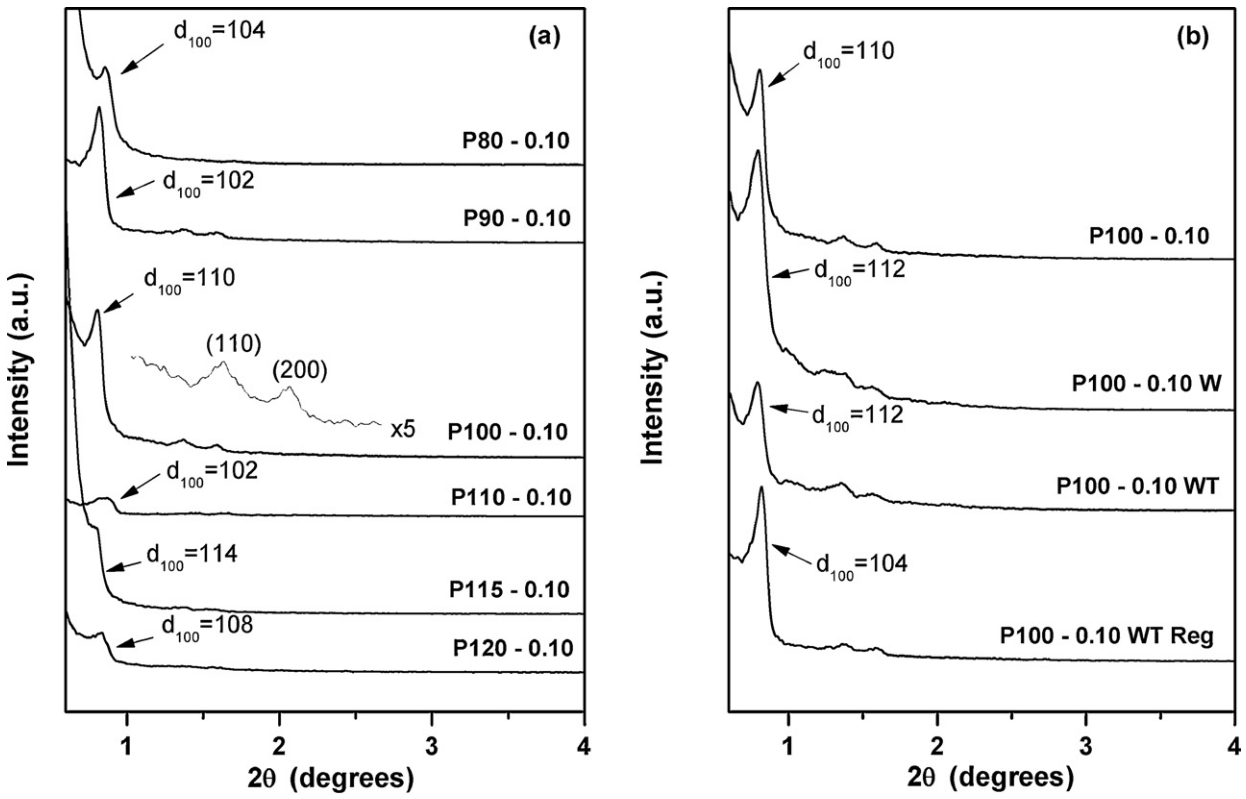

Fig. 3. XRD data of the propylsulfonic series (a) and the stability of used and regenerated P100-0.10 sample (b).

Table 3
Catalytic activity of functionalized SBA-15 for different P100 propylsulfonic loads and different reaction temperatures.

P100 sulfonic load		Batchwise in water[a,b]				Batchwise in toluene/water[a,b]			
Sample	Acidity[c]	X_X[d] (%)	FUR_S[e] (%)	FUR_Y (%)	TOF[f] (mmol (meq H^+)$^{-1}$ h^{-1})	X_X[d] (%)	FUR_S[e] (%)	FUR_Y (%)	TOF[f] (mmol (meq H^+)$^{-1}$ h^{-1})
P100-0.05	0.44	49	55	26	1.23	45	60	27	1.13
P100-0.10	1.04	64	60	38	0.68	67	82	55	0.71
P100-0.20	1.69	73	80	58	0.48	71	89	63	0.66

Temperature effect		Batchwise in toluene/water[b]		
Sample	Reaction T (°C)	X_X[d] (%)	FUR_S[e] (%)	FUR_Y (%)
P80-0.10	140	61	65	40
	155	92	69	63
	170	95	73	69
P100-0.10	140	67	82	55
	155	81	81	66
	170	96	85	82
P120-0.10	140	73	62	45
	155	82	73	66
	170	96	66	68
A100-0.10	140	63	60	38
	155	85	65	55
	170	99	72	71
Amberlyst 70	140	65	49	32
	155	85	62	53
	170	99	40	40

[a] Catalytic test at 140 °C of reaction temperature.
[b] Reaction conditions: 200 mL, 2 wt.% xylose loading and 60 wt.% catalyst loading with respect to initial xylose. $SD_{TOL/W}$ = 5%, SD_{DMSO} = 3%.
[c] Measured by TMACl equilibration followed by titration with NaOH.
[d] Conversion of xylose after 20 h.
[e] Selectivity to FUR after 20 h.
[f] Turnover frequency calculated after 20 h of reaction.

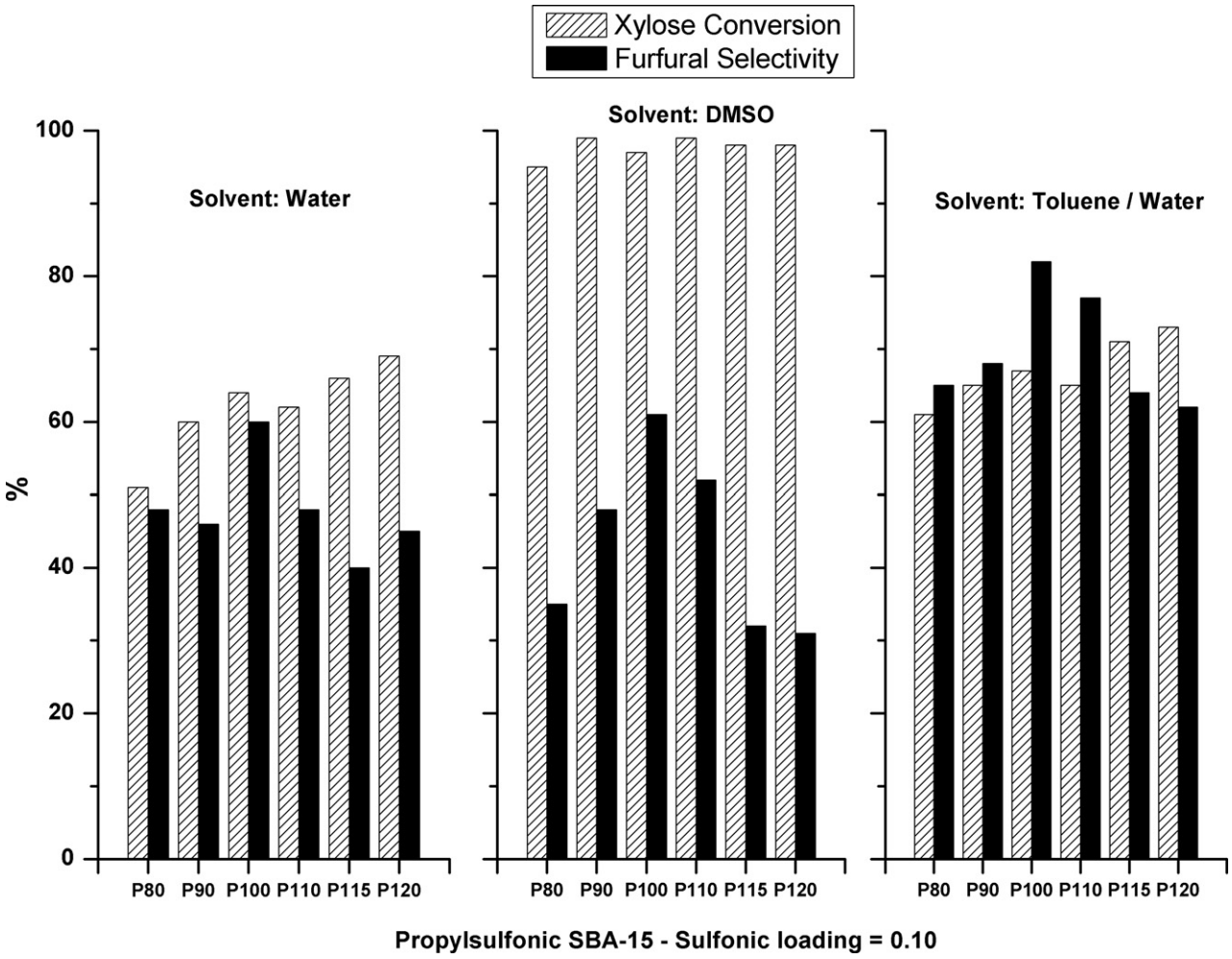

Fig. 4. Catalytic xylose conversion and furfural selectivity of the propylsulfonic samples in water, DMSO and toluene/water (1/1, v/v).

active sites. This higher activity could be due to lower disturbances generated by other neighbor sites or due to increasing interaction between the sulfonic group and the silica surface when lower amount of acid sites were anchored to it. On the other hand, overall conversion and selectivities are the result of the combination of the acid sites number and the activity showed by each site.

The xylose dehydration activity showed a proportional relation to the sulfonic loading. This is a clear indication that the effect of an increase of the acid site number is higher than the effect of a decrease of each acid site activity. Higher loads converted xylose at faster rates. However, there was considerable difference in the FUR_S values. P100-0.20 clearly achieved higher FUR_S both in water and toluene/water systems (80% and 89%, respectively). During the incorporation of sulfonic precursors on the mesophase formation, P100-0.20 sample still showed higher capacity for sulfonic incorporation than the one in P100-0.10. This way, pores got saturated by the sulfonic sites. The FUR_S values obtained in water-phase systems are comparable to more sophisticated solvents such as DMSO [14] or complex functionalized porous structures [18].

3.4. Temperature effect

Reaction temperature has been proved as a relevant variable in order to find an equilibrium between xylose dehydration and secondary reactions. Low temperatures require strong Brönsted acid catalysts in order to convert xylose, while the conversion rate is exponentially increased with temperature. Over 175 °C, the system is sufficiently autocatalyzed by the H_3O^+ in the water and secondary reactions are minimized by the so-called "entropy effect" [42].

In this study, propylsulfonic catalysts were tested over three different temperatures. Table 3 summarizes the conversion and selectivity values of propylsulfonic materials compared to A100-0.10 and Amberlyst 70. There was clear evidence of the temperature effect on the xylose dehydration rate over all the studied samples. The series from P80 to P120 showed clear evidences that higher reaction temperatures increased the diffusion of xylose to the acid sites. Higher conversion rates were obtained from a combination of faster xylose dehydration and xylose + furfural condensation reactions. Over 140 °C, homogeneous liquid-phase reaction played an important role, contributing to part of xylose conversion. Moreover, catalysts such as Amberlyst 70, containing more acid surfaces, could reach almost 100% X_X at 170 °C. Among the sulfonic functionalized materials, A100-0.10 material showed a similar tendency as its propyl analog. However, except for 140 °C, A100-0.10 X_X values are the same as P100-0.10. This might be attributed to higher sulfonic site stability of the arylic ring compared to the propyl chain for reactions at 155 and 170 °C (see Section 3.5). The molecular diffusion effects were here checked for the propylsulfonic series. Even if experimental data present different xylose conversion rates, D_K effects slightly changed for P80 (0.033 and 0.035 cm^2/s for 140 and 170 °C, respectively).

FUR_S values showed a similar increasing tendency as the xylose conversion values, except for P120-0.10 and Amberlyst 70. In these cases, the high pore accessibility of P120-0.10 at high temperatures

(170 °C) led to faster secondary reactions than to FUR production. On the other hand, the pore size of P100-0.10, A100-0.10 and P80-0.10 seemed to be selective enough to optimize the FUR_Y over the whole temperature range. The FUR_S improvement at 170 °C, measured in relation to the FUR_S at 140 °C, is most significant for P80-0.10 (12%) and for A100-0.10 (20%). Highest FUR_S values of 85% are achieved for P100-0.10 at 170 °C, with a FUR_Y of 82%. The catalytic results obtained in this study are comparable to the study performed at 160 °C using propylsulfonic SBA-15, obtaining a FUR_Y of 66% [36]. As an example, coated MCM41-SO_3H obtained maximum FUR_Y of ~80% under biphasic toluene/water conditions at 170 °C [14].

3.5. Stability of functionalized SBA-15 materials

TGA data were used as a check for sulfonic site stability under oxidative conditions (see Fig. 2). Arenesulfonic SBA-15 materials showed higher thermal stability than propylsulfonic ones (desorption peak at 490 °C), with one peak centered at 500 °C and an adjacent one at 585 °C. The sulfonic groups present in the P100P-0.10 sample (not represented here) showed considerably less stability since they were decomposed at 270 °C. However, functionalized SBA-15 samples did not achieve the same stability behavior under the hydrothermal conditions during xylose dehydration. According to TGA, 75% of all propylsulfonic acid sites were completely leached at 140 °C from the silica matrix after 20 h of reaction (Fig. 2). This deactivation occurred gradually during the whole reaction time. After 20 h, the surface still showed some acidity. In order to follow the catalyst deactivation, some shorter experiments were also carried out and it was proved that 67% of the total xylose conversion occurred in the first 6 h of reaction, where 60% of initial acid sites were still not leached. Even if the high electron density of the aryl ring strengthens the silica–sulfonic bond, A100-0.10 sites showed similar stabilities than P100-0.10.

TEM analysis (not shown here) confirmed the presence of decomposition products adsorbed on the mesopore surface as a consequence of xylose and furfural secondary reactions in contact with the sulfonic acid sites. These are decomposed at 250–300 °C. Acid capacities were also reduced from ~1.0 to 0.3 mmol H^+/g SiO_2 for P100-0.10 and to 0.4 mmol H^+/g SiO_2 for A100-0.10. Melero et al. [35] proved that even boiling-water reduces the acid capacity of arenesulfonic materials about 50%, whereas organic solvents preserve the sulfonic sites for contact times as long as 70 h.

In order to clarify the hydrolytic attack of water during stability tests, the propylsulfonic functionalized materials were tested under the same conditions in methanol and DMSO as solvent. As observed in Fig. 2, methanol, due to a smaller dielectric constant (DC) than water (DC_{MET} = 33, DC_{WATER} = 80), gave higher sulfonic stability. However, DMSO (DC = 47) showed complete sulfonic acid site preservation after the xylose dehydration reaction at 140 °C. This difference was also reasoned by the acid capacity of each solvent. DMSO shows a pK_a value of 35, while the pK_a values for water and methanol are around 15. As a result, the acidity of water and methanol enhanced the cleavage of silica–propylsulfonic bond at 140 °C, and thus the sulfonic sites became less stable.

Structural stability of used sulfonic materials was also checked by N_2 physisorption. Propylsulfonic catalysts were filtrated from the reaction medium and washed with ethanol and water in order to remove weakly absorbed oligomers. The surface area was considerably reduced after the reaction in water (513 m^2/g) and in toluene/water (765 m^2/g). The high reaction temperature created such aggressive conditions that silanol groups were dehydrated to siloxane, leading to strong structural shrinkage. Non-functionalized SBA-15 materials proved high hydrothermal stability under boiling water conditions [43,44]. However, xylose dehydration reactions at 140 °C might be more aggressive. XRD data (Fig. 3b), confirmed by TEM analysis, showed that the initial crystallinity of P100-0.10 was preserved after the reaction. The shift of the (1 0 0) reflection to the right side was also due to the mesopore shrinkage.

3.6. Regeneration of propylsulfonic SBA-15 catalyst

In order to regenerate the used propylsulfonic materials, the used materials were oxidized with H_2O_2. In a typical experiment, 0.3 g of dry used material were suspended in 10 mL of 30 wt.% H_2O_2, stirred for 8 h at room temperature, filtered and dried. This way, the oligomers present at the silica surface, giving the brown color to the used materials, were completely removed. The catalysts turned back to the initial white color. TGA analysis of as-treated materials showed a complete disappearance of deposited products. This procedure allowed to recover the initial structural properties of P100-0.10 (fresh materials in Table 2) tested in toluene/water (V_P = 1.74 cm^3/g and Main D_P = 74.6 Å), except for the S_{BET} (776 m^2/g). As observed in Fig. 3b, the XRD pattern at the (1 0 0) reflection of regenerated P100-0.10 showed a slight shift to the right ($2\theta = 0.79°$ for P100-0.10 WT and $2\theta = 0.81°$ for P100-0.10 WT Reg). This shift was caused by the structural shrinkage during the harsh oxidizing conditions with H_2O_2. However, these conditions preserved the initial crystallinity of P100-0.10. Following the d_{100} spacing data, this slight structural changes resulted in a reduction of interpore distance and thus thinner wall thickness.

The regeneration procedure removed almost all secondary products and preserved most of the initial structural properties, but the initial sulfonic properties could not be recovered. According to the TMACl equilibration method, the regeneration of P100-0.10 WT could increase its acid capacity from 0.30 to 0.40 mmol H^+/g SiO_2. This suggested that the acid sites of used materials were blocked by oligomers during acidity analysis. The catalytic activity of regenerated P100-0.10 was also tested. The X_X of used P100-0.10 at 140 °C was decreased from 67% to 34 and 33% for 1st and 2nd run, respectively. FUR_S was also reduced to 37 and 35%, respectively.

4. Concluding remarks

The present study concludes that functionalized SBA-15 materials are very suitable catalysts for the cyclodehydration of xylose to furfural. The combination of controlled textural properties with propylsulfonic acid sites resulted in very promising materials to selectively produce furfural. This study reveals that final FUR_Y is directly related to the diffusion of xylose and furfural on the porous structure of materials aged from 80 to 120 °C. The material prepared at 100 °C achieved the highest FUR_S of 85% for 96% of xylose conversion at 170 °C of reaction temperature. Moreover, high FUR_S values were obtained for P100-0.20 in water-phase conditions. Sulfonic acid site content was decreased after these reactions, but they showed high structural stability. Finally, oligomers on the catalyst surface could be completely removed by H_2O_2 regeneration. In order to improve the sulfonic site stability of SBA-15 catalysts, current work is focused on preparing functionalized SBA-15 supports by using highly stable surfactants. This procedure allows to synthesize catalysts at temperatures up to 190 °C. Under these conditions, the silica–sulfonic interaction should be strong enough to create more stable materials for the studied reaction temperatures.

Acknowledgments

This work was supported by funds from the Ministerio de Ciencia e Innovación ENE2009-12743-C04-04 and from the Gobierno Vasco (Programa de Formación de Personal Investigador del Departamento de Educación, Universidades e Investigación). The authors

also gratefully acknowledge Dow Chemical for kindly supplying the Amberlyst 70 catalyst.

Appendix A. Supplementary data

Supplementary data associated with this article can be found, in the online version, at doi:10.1016/j.apcatb.2011.12.025.

References

[1] A. Corma, S. Iborra, A. Velty, Chem. Rev. 107 (2007) 2411–2502.
[2] H.D. Mansilla, J. Baeza, S. Urzua, G. Maturana, J. Villasenor, N. Duran, Bioresour. Technol. 66 (1998) 189–193.
[3] R. Weingarten, J. Cho, W.C.J. Conner, G.W. Huber, Green Chem. 12 (2010) 1423–1429.
[4] K.J. Zeitsch, Sugar Series, vol. 13, first ed., Elsevier, The Netherlands, 2000, p. 1.
[5] A.S. Dias, M. Pillinger, A.A. Valente, Appl. Catal. A 285 (2005) 126–131.
[6] M. Vazquez, M. Oliva, S.J. Tellez-Luis, J.A. Ramirez, Bioresour. Technol. 98 (2007) 3053–3060.
[7] S. Lima, M.M. Antunes, A. Fernandes, M. Pillinger, M.F. Ribeiro, A.A. Valente, Appl. Catal. A 388 (2010) 141–148.
[8] A.S. Mamman, J.M. Lee, Y.C. Kim, I.T. Hwang, N.J. Park, Y.K. Hwang, J.S. Chang, J.S. Hwang, Biofuels Bioprod. Biorefin. 2 (2008) 438–454.
[9] I. Agirrezabal-Telleria, A. Larreategui, J. Requies, M.B. Güemez, P.L. Arias, Bioresour. Technol. 102 (2011) 7478–7485.
[10] T. Okuhara, Chem. Rev. 102 (2002) 3641–3665.
[11] R. Rinaldi, F. Schuth, Energy Environ. Sci. 2 (2009) 610–626.
[12] A. Chareonlimkun, V. Champreda, A. Shotipruk, N. Laosiripojana, Bioresour. Technol. 101 (2010) 4179–4186.
[13] A.S. Dias, S. Lima, D. Carriazo, V. Rives, M. Pillinger, A.A. Valente, J. Catal. 244 (2006) 230–237.
[14] A.S. Dias, M. Pillinger, A.A. Valente, J. Catal. 229 (2005) 414–423.
[15] A.S. Dias, M. Pillinger, A.A. Valente, Microporous Mesoporous Mater. 94 (2006) 214–225.
[16] A.S. Dias, S. Lima, P. Brandao, M. Pillinger, J. Rocha, A.A. Valente, Catal. Lett. 108 (2006) 179–186.
[17] A.S. Dias, S. Lima, M. Pillinger, A.A. Valente, Catal. Lett. 114 (2007) 151–160.
[18] S. Lima, A. Fernandes, M.M. Antunes, M. Pillinger, F. Ribeiro, A.A. Valente, Catal. Lett. 135 (2010) 41–47.
[19] C. Moreau, R. Durand, D. Peyron, J. Duhamet, P. Rivalier, Ind. Crop. Prod. 7 (1998) 95–99.
[20] C. Perego, A. Bosetti, Microporous Mesoporous Mater. 144 (2011) 28–39.
[21] F. Hoffmann, M. Cornelius, J. Morell, M. Fröba, Angew. Chem. Int. Ed. 45 (2006) 3216–3251.
[22] D. Zhao, J. Feng, Q. Huo, N. Melosh, G.H.M. Fredrickson, B.F. Chmelka, G.D. Stucky, Science 279 (1998) 548–552.
[23] P. Feng, X. Bu, D.J. Pine, Langmuir 16 (2000) 5304–5310.
[24] M. Colilla, F. Balas, M. Manzano, M. Vallet-Regi, Chem. Mater. 19 (2007) 3099–3101.
[25] A. Galarneau, H. Cambon, F. Di Renzo, F. Fajula, Langmuir 16 (2001) 8328–8335.
[26] P.I. Ravikovitch, A.V. Neimark, J. Phys. Chem. B 105 (2001) 6817–6823.
[27] A. Galarneau, H. Cambon, F. Di Renzo, R. Ryoo, M. Choib, F. Fajula, New J. Chem. 27 (2003) 73–79.
[28] C. He, Q. Li, P. Li, Y. Wanga, X. Zhanga, J. Chenga, Z. Haoa, Chem. Eng. J. 162 (2010) 901–909.
[29] P. Bhange, D.S. Bhange, S. Pradhan, V. Ramaswamy, Appl. Catal. A: Gen. 400 (2011) 176–184.
[30] J.J. Zhu, X.A. Xie, S.A.C. Carabineiro, P.B. Tavares, J.L. Figueiredo, R. Schomacker, A. Thomas, Energy Environ. Sci. 4 (2011) 2020–2024.
[31] S. Miao, B.H. Shanks, Appl. Catal. A: Gen. 359 (2009) 113–120.
[32] J.A. Melero, L.F. Bautista, G. Morales, J. Iglesias, R. Sanchez-Vazquez, Chem. Eng. J. 161 (2010) 323–331.
[33] A.J. Crisci, M.H. Tucker, M.Y. Lee, S.G. Jang, J.A. Dumesic, S.L. Scott, ACS Catal. 1 (2011) 719–728.
[34] X. Shi, Y. Wua, P. Li, H. Yi, M. Yang, G. Wang, Carbohydr. Res. 346 (2011) 480–487.
[35] J.A. Melero, G.D. Stucky, R. Van Griekena, G. Moralesa, J. Mater. Chem. 12 (2002) 1664–1670.
[36] X. Shi, Y. Wu, H. Yi, G. Rui, P. Li, M. Yang, G. Wang, Energies 4 (2011) 669–684.
[37] D. Margolese, J.A. Melero, S.C. Christiansen, B.F. Chmelka, G.D. Stucky, Chem. Mater. 12 (2000) 2448–2459.
[38] D.E. Resasco, G.L. Haller, Catalysis, Royal Society of Chemistry, 1994.
[39] A. Sayari, Y. Yang, Chem. Mater. 17 (2005) 6108–6113.
[40] J.M. Smith, Chemical Engineering Kinetics, 3rd ed., McGraw-Hill, 1981.
[41] R. O'Neill, M.N. Ahmad, L. Vanoye, F. Aiouache, Ind. Eng. Chem. Res. 48 (2009) 4300–4306.
[42] A.S. Dias, S. Lima, M. Pillinger, A.A. Valente, Ideas in Chemistry and Molecular Sciences: 3 Volume Set: Advances in Synthetic Chemistry–Where Chemistry Meets Life–Advances in Nanotechnology, Materials and Devices, Part III, Wiley, 2010, pp. 165–186.
[43] M. Kruk, M. Jaroniec, Chem. Mater. 12 (2000) 1961–1968.
[44] M. Impéror-Clerc, P. Davidson, A. Davidson, J. Am. Chem. Soc. 122 (2000) 11925–11933.